Journal of Power Sources 244 (2013) 395–402

Contents lists available at SciVerse ScienceDirect

Journal of Power Sources

journal homepage: www.elsevier.com/locate/jpowsour

Facile synthesis of ZrO_2 coated Li_2CoPO_4F cathode materials for lithium secondary batteries with improved electrochemical properties

S. Amaresh [a], K. Karthikeyan [a], K.J. Kim [a], M.C. Kim [a], K.Y. Chung [b], B.W. Cho [b], Y.S. Lee [a,*]

[a] Faculty of Applied Chemical Engineering, Chonnam National University, Gwangju 500-757, Republic of Korea
[b] Center for Energy Convergence, Korea Institute of Science and Technology, Seoul 136-791, Republic of Korea

HIGHLIGHTS

- A highly durable ZrO_2 coating was applied to 5 V class cathode material Li_2CoPO_4F.
- The 5 wt% ZrO_2 coated sample exhibited highest discharge capacity of 144 mA h g^{-1}.
- 5 wt% samples exhibited higher capacities at 10–500 mA g^{-1} current rates.
- The durability of Li_2CoPO_4F increased to 70% after coating even at 100 mA g^{-1} rate.

ARTICLE INFO

Article history:
Received 5 October 2012
Received in revised form
1 December 2012
Accepted 3 December 2012
Available online 12 December 2012

Keywords:
Cobalt fluorophosphate
Cathode material
Zirconium oxide
Coating
Lithium battery

ABSTRACT

A facile synthesis of a metal oxide (ZrO_2) coating on the surface of high voltage type Li_2CoPO_4F cathode material using the conventional solution method is reported in this study. The Li_2CoPO_4F is prepared by a two step solid state method, followed by the application of wet coating containing various amounts of ZrO_2. Among the samples, the 5 wt% ZrO_2 coated Li_2CoPO_4F material shows the best performance with an initial discharge capacity of up to 144 mA h g^{-1} within the voltage range of 2–5.2 V vs Li at 10 mA g^{-1}. Moreover, this ZrO_2 coated cell demonstrates an enhanced capacity retention which is two times higher than that of the uncoated sample. The reversible extraction–insertion of one lithium unit from Li_2CoPO_4F is successfully carried out in a controlled environment, where the electrolyte decomposition is reduced using a highly durable ZrO_2 coating. The nanosized coating over the Li_2CoPO_4F surface helps to attain a higher discharge capacity even at high current rates. As a consequence, the cell delivers a capacity of 104 mA h g^{-1} at a high current rate of 100 mA g^{-1}.

1. Introduction

The increasing awareness of environmental protection and the ever increasing demand for energy in all sectors, particularly in electronics and automobiles, have created the need to develop alternative energy sources. Batteries have evolved as a favorite source of energy storage and utilization ever since their discovery. Among the various battery chemistries like lead-acid, nickel metal hydride, etc., lithium ion batteries have emerged as the most suitable candidate to meet the energy requirements for future applications. The lithium ion battery market has been growing since its inception in 1990 through the commercialization of $LiCoO_2$ cathodes and is now expected to grow to over 40 billion dollars by 2020 [1–3]. This target was formulated based on the existing cathodes, while the search for energy efficient materials is still in progress. A class of cathode materials which have garnered immense attention over the past two decades is olivine phosphates; $LiMPO_4$ (M = Co, Fe, Mn). The phosphates have enhanced capacity, high stability and improved safety characteristics, hence, $LiMPO_4$ active materials have secured a primary position as the next generation energy source materials [4]. Nevertheless, the desire for energy grew when products such as arrays of electric vehicles were conceptualized. In this connection, fluorophosphate cathode materials containing twice the amount of lithium as that of olivine phosphates have been postulated [5–12]. The charge compensation for the additional lithium ion was achieved with highly electronegative fluorine in an attempt to increase the stability and double the capacity by utilizing two intercalating lithium ions. Fluorophosphate cathode materials with the general formula A_2MPO_4F (where A = Na, Li and M = Co, Mn, Fe, Ni, Cr) have a stable structure with the phosphate polyanion group together with

* Corresponding author. Tel./fax: +82 62 530 1904.
E-mail address: leeys@chonnam.ac.kr (Y.S. Lee).

0378-7753/$ – see front matter © 2012 Elsevier B.V. All rights reserved.
http://dx.doi.org/10.1016/j.jpowsour.2012.12.010

the highly electronegative fluoride ion. Among them, the lithium cobalt fluorophosphate (i.e. Li_2CoPO_4F) cathode, with a theoretical capacity for two lithium intercalation reaction is as high as 300 mA h g^{-1}, has been shown to be a promising candidate for electric vehicles (EVs) and plug-in hybrid electric vehicles (PHEVs). This high capacity and high voltage of operation would make Li_2CoPO_4F useful in the EV industry, provided the material is operated at maximum usage. The structure and electrochemical characteristics of Li_2CoPO_4F as a promising 5 V cathode for lithium ion batteries was first reported by Okada *et al.* [13]. There have been attempts to produce high purity Li_2CoPO_4F material with a shorter synthesis time in order to extract a higher percentage of lithium and maximize the capacity within the operating voltage of the currently available electrolytes [14]. In spite of all these efforts, only 30% of the available capacity has been recovered. Also, high voltage operation affected the surface of the cathode materials and degraded their intrinsic properties. Metal dissolution into the electrolytes has also been observed for Li_2CoPO_4F materials. The oxidation of the electrolyte played a vital role in decreasing the operating capability of the fluorophosphate cathode materials, with the high voltage operation being the main reason for the decomposition of the electrolyte species.

The surface of cathode materials forms major active sites for the above-mentioned parasitic reactions. It is of paramount importance to reduce these active spots and prevent adverse side reactions. Also, the development of highly stable, low cost electrolytes for stable battery operation above 4.8 V and their commercialization is not to be expected in the near future. On the other hand, the application of metal oxide coatings, such as ZrO_2 [15,16], Al_2O_3 [17,18], TiO_2 [19,20], MgO [21,22] and ZnO [23–25], over the surface of cathode active materials, which is considered to be one of the best methods of improving their electrochemical stability, has been attempted to overcome the problem of electrolyte decomposition. In general, most surface treatments have a positive impact on the electrochemical properties of electrode materials. It is also noted that they have advantageous effects on the former intercalation compounds such as $LiNiO_2$ and $LiCoO_2$, which have limited capacity utilization due to electrolyte oxidation factor [15,26]. These surface coatings act as an inert layer between the electrode material and electrolyte, especially against the HF which forms during cycling. Coatings based on zirconium presented the best capacity retention capability during cycling above 4.5 V, due to their non-destructible property even at high rate operation. ZrO_2 coated materials have also been shown to offer high temperature storage properties and to increase the stability of $LiMn_2O_4$ during the cycle life performance test at 55 °C [27]. The effective suppression of lattice constants during charging, retention of open circuit voltage after prolonged storage and the reduction of metal dissolution in the case of cathode materials such as $LiCoO_2$ and $LiNiO_2$ have made the use of such nanoscale ZrO_2 coatings the preferred choice for protecting cathode surface, especially for cathodes with higher operating potentials. In this regard, ZrO_2 was chosen for coating the surface of Li_2CoPO_4F to improve its electrochemical performance. Inert oxides can enhance the interphase stability between the electrolyte and electrode in charged state, since the direct contact of electrode and electrolyte is restricted. Also, these oxides can reduce the structural breakage and decrease the side reactions with the electrolyte on the surface of the cathode.

In this study, the effect of coatings with different mass percents of ZrO_2 on the surface of Li_2CoPO_4F cathode materials was examined. The cathode active material was synthesized by a simple solid state method followed by the wet coating of an oxide film over its surface. To the best of our knowledge, this is the first attempt to employ a metal oxide to improve the electrochemical properties of framework cobalt fluorophosphate cathode materials. XRD, SEM, TEM and the cycling test were employed to study the structural, morphological and electrochemical characteristics of the ZrO_2 coated Li_2CoPO_4F cathode materials systematically and the results are discussed in detail.

2. Experimental

Li_2CoPO_4F powders were synthesized by the conventional two step solid state method. The starting materials, lithium hydroxide monohydrate (Junsei, Japan), cobalt(II,III) oxide (Alfa Aesar, USA) and ammonium phosphate dibasic (Sigma–Aldrich, USA), were stoichiometrically weighed and intimately mixed using a planetary ball mill. The resultant mixture was pelletized and then annealed at 400 °C and 800 °C to yield $LiCoPO_4$ in air atmosphere for 10 h each. The $LiCoPO_4$ powders were reground thoroughly with LiF (Wako, Japan) using a mortar and pestle and then pelletized. The pellet was slowly heated at 5 °C min^{-1} under an argon atmosphere and finally quenched to room temperature after 1.5 h of exposure at 700 °C. Quenching allowed the Li_2CoPO_4F particles to retain their composition, which would otherwise be decomposed into $LiCoPO_4$ and LiF along with some other impurities phases such as CoO and Li_3PO_4 if cooled slowly [29,39]. The heating time for final sintering was optimized such that the decomposition of Li_2CoPO_4F was avoided and thus a phase pure Li_2CoPO_4F was prepared.

To prepare ZrO_2 coated Li_2CoPO_4F, the acetate salt of zirconium, namely zirconium(IV) acetate hydroxide (Sigma–Aldrich, USA), was first dissolved in water and stirred constantly at 50 °C. The surface of the synthesized Li_2CoPO_4F powders was prepared by sonication for 0.5 h and then the mixture was added to the coating solution, maintaining vigorous stirring for the subsequent 24 h. The final amount of coating materials in the mixture was fixed at 1, 3, 5 and 7 wt% of the initial starting materials. The mixture was dried at 60 °C and finally fired at 500 °C for 5 h in an air atmosphere. During the preparation of the pristine and ZrO_2 coated samples, no materials related to the formation of carbon were used. The surface area of the samples was analyzed using a surface area analyzer (ASAP2020, Micromeritics, USA). A heating rate of 10 °C min^{-1} was maintained throughout the synthesis unless specified.

X-ray diffraction studies (XRD, Rint 1000, Rigaku, Japan), Fourier transform infrared spectroscopy (FTIR, IRPresitge-21, Shimadzu, Japan), field emission scanning electron microscopy (FE-SEM, S-4700, Hitachi, Japan) and transmission electron microscopy (TEM, TECNAI, Philips, Netherlands) were employed to verify the structure and morphology of the pristine and coated Li_2CoPO_4F samples. Electrochemical characterizations of all the synthesized materials were performed using a CR2032 coin cell fabricated in a glove box under a controlled atmosphere. The cell consisted of the synthesized material as the cathode and a metallic lithium anode separated by a polypropylene separator with 1 M $LiPF_6$ dissolved in 1:1 EC:DMC by volume as the electrolyte. The cathodes were prepared with 20 mg of active material, 3 mg of Ketzen black (KB) and 3 mg of teflonized acetylene black (TAB) over a stainless steel current collector, followed by drying at 160 °C for 4 h before the fabrication of the cell. Galvanostatic charge/discharge testing using a battery tester (WBCS 3000, Won-A-Tech, Korea) was used to evaluate the electrochemical performance of the pristine and ZrO_2 coated Li_2CoPO_4F cathode materials. Electrochemical impedance spectroscopy and cyclic voltammetry studies were carried out with the cell as constructed above using an electrochemical work station (SP-150, Bio-Logic, France).

3. Results and discussion

The X-ray diffraction data obtained between 10 and 55° at a step increment of 0.02° for the pristine and coated samples are presented in Fig. 1. It is seen that there are no evident impurity phases such as $LiCoPO_4$, CoP_3, and Li_3PO_4 unlike those observed by Wang

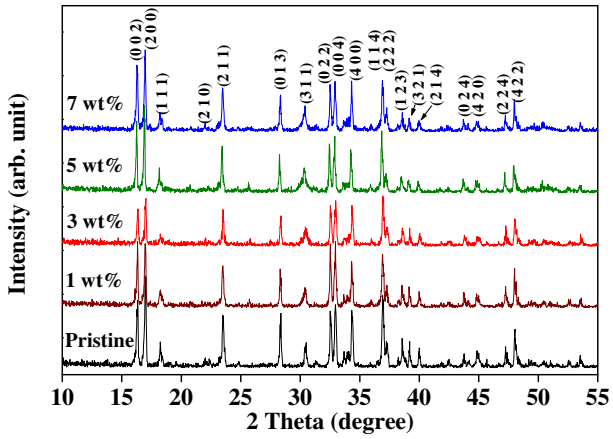

Fig. 1. Powder XRD patterns of Li_2CoPO_4F coated with various amounts of ZrO_2. (a) Pristine, (b) 1 wt%, (c) 3 wt%, (d) 5 wt%, and (e) 7 wt%.

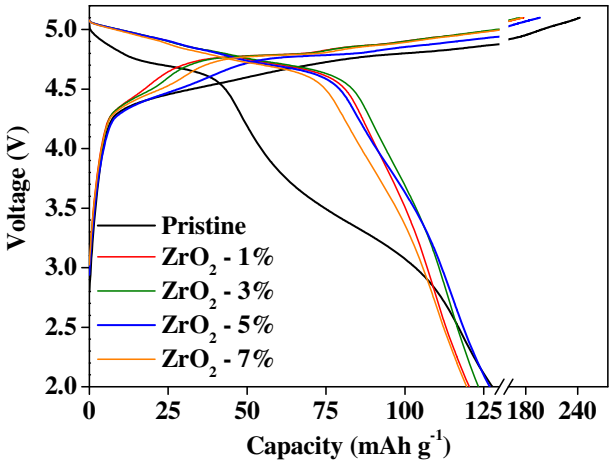

Fig. 2. The initial charge/discharge characteristics of the cells containing the pristine Li_2CoPO_4F and Li_2CoPO_4F cathode materials coated with various amounts of ZrO_2 cycled between 2 and 5.1 V vs Li at 10 mA g^{-1}.

et al. [28] for coated samples. Consequently, the XRD patterns were indexed based on an orthorhombic structure with *Pnma* space group and were found to match well with JCPDS 56-1493 and earlier reports [14,29]. The coated samples were heated at 500 °C to ensure the removal of the solvent used and the formation of an oxide layer over the surface of Li_2CoPO_4F. Since the temperature maintained after coating was close to the synthesis temperature of the Li_2CoPO_4F material, it was suspected that the heating would affect its inherent structure. The absence of additional impurities for the coated samples revealed that the coating modified the surface of the active material and did not alter the bulk properties of the parent active material. In contrast, the pristine material developed peaks corresponding to secondary phases such as $LiCoPO_4$ and Li_3PO_4 when heated at 500 °C. Apparently, there was no peak broadening or additional peaks for crystalline ZrO_2 found in the XRD pattern, as observed in the case of the ZrO_2 coated $LiNiO_2$ cathode material [15]. It is, therefore, assumed that the coating is either amorphous or too thin to be observed by XRD. A decrease in the peak intensity for the coated samples was observed, irrespective of the amount of coating materials, which may be due to the thermal stress caused by the additional heating carried out after the coating process. Additionally, the decrease in intensity for the 1 and 3 wt% samples were comparatively higher than those of the other coated samples which had almost the same intensities as those of the pristine material, which may be due to the insufficient amount of coating materials covering the surface of the Li_2CoPO_4F particles [30].

In order to study the electrochemical performance of the pristine and surface coated Li_2CoPO_4F active materials, CR2032 coin cells were tested between 2 and 5.1 V at a constant current density of 10 mA g^{-1} in constant current charge/discharge mode. The initial charge/discharge curves of the pristine and modified Li_2CoPO_4F samples coated with different weight percentages of ZrO_2 are presented in Fig. 2. The discharge capacity obtained was 128 mA h g^{-1} for the pristine Li_2CoPO_4F and 121, 123, 127 and 120 mA h g^{-1} for the samples coated with 1, 3, 5 and 7 wt% of ZrO_2, respectively. It is evident that the discharge capacity increased with increasing amount of coating material for the Li_2CoPO_4F powders until it reached 5 wt% and then decreased for the 7 wt% sample, but which was a very small change that can be neglected. Since the electrolyte used has a voltage limitation and the report from Wang *et al.* [28] suggested that only one lithium ion was extracted up to 5.5 V vs Li, the excessive charging capacity for both the pristine and coated samples can be ascribed to the decomposition that occurs due to the thermodynamic instability of the electrolyte at voltages close to 5 V and the contribution of this decomposition reaction during charging at a low current rate [31], such as C/12 in this case. It is worth noting here that the additional capacity was decreased to an average of 60 mA h g^{-1} in the case of the coated samples compared to the charging capacity of the pristine Li_2CoPO_4F cell. In spite of delivering a reduced charging capacity, the cells with the ZrO_2 coated samples exhibited a discharge capacity close to that of the pristine sample, which means that the irreversible capacity loss that occurred for the uncoated sample was reduced in the case of the ZrO_2 coated Li_2CoPO_4F ones. Hence, it is understood that the coating does not alter the inherent structural properties of the Li_2CoPO_4F active material. The Co metal dissolution that occurs at high voltages, which is the main reason for the reduction in potential and occurred to a greater extent for the Li_2CoPO_4F samples without the protective coating, is thus reduced by the presence of a thin layer of ZrO_2 covering the cathode active material. In addition, the maximum discharge capacities achieved for the pristine and coated samples, when charged up to 5.1 V vs Li, were in the range of 82–90% of the theoretical capacity (calculated based on one lithium intercalation reaction) and all the values were higher than the highest capacity reported for Li_2CoPO_4F cathode materials [13,14,29].

The monotonous nature of the charge/discharge curves for both the pristine and coated active materials indicated the absence of a two phase reaction, unlike in the case of the $LiCoPO_4$ cathode materials. However, the two stage lithium extraction was observed more clearly for the ZrO_2 coated samples than for the pristine material. During charging, the coated sample had a narrow plateau at 4.4 V, irrespective of the amount of ZrO_2 used, followed by a long linear plateau at 4.8 V corresponding to the $Co^{2+/3+}$ redox process. The charge/discharge operating plateau of all of the coated materials was also increased compared with that of the pristine Li_2CoPO_4F. Also, the uncoated sample exhibited solid solution like behavior during discharge up to 4.8 V and then the decreasing plateau of discharge profile sustained till the extraction of 0.35 Li^+ ions, calculated based on a total of one lithium extraction, while the plateau for the coated samples was extended till the extraction of 0.6 Li^+ ions; that is, the retention of the ZrO_2 coated cells was twice that of the uncoated samples. The phenomenon underlying the enhanced performance of the ZrO_2 coated cells can be explained as follows: the coating layer acts as a buffer layer between the Li_2CoPO_4F and acidic species formed during cycling in the standard electrolyte based on $LiPF_6$, yet allowed the smooth movement of Li

ions during intercalation [15,16,26,27]. This led to the increase in participation of the active mass for intercalation, thereby maximizing the surface area of the active materials and, thus, increasing the operating plateau [15,26]. In other words, the poor performance of the pristine sample is due to the surface erosion by the electrolyte decomposition products during both the charge and discharge processes, leading to the change in nature of the active material even after the first cycle.

After the initial discharge cycle at C/12, the rate performance of the cells was tested at various current rates, namely C/2, 1 C, 2 C, 5 C and 7 C, and the results are shown in Fig. 3(a). The cells were charged at 25 mA g^{-1} and then discharged at the various current rates mentioned above, except for the initial C/12 rate where the charge and discharge are done at 10 mA g^{-1}. The results clearly indicated that the 5 wt% ZrO_2 coated Li_2CoPO_4F performed well with higher discharge capacity at all current rates than that obtained for the pristine and coated samples. The discharge capacities obtained in the case of the 5 wt% ZrO_2 coated sample were 113, 101, 93, 83 and 76 mA h g^{-1} at current rates of C/2, 1 C, 2 C, 5 C and 7 C, respectively. The rate performances of the pristine and 5 wt% ZrO_2 coated samples were further studied for 3 consecutive cycles and the performance of the cells at current rates as high as 500 mA g^{-1} (7 C) was observed (Fig. 3(b)). The increase in the discharge capacity for the 5 wt% ZrO_2 coated cell at low current rates such as C/12 and C/2 was minimal, but as the current density increased, the retention in capacity increased, reaching almost twice that of the uncoated sample at higher current rates.

It is well known that the oxidation of the electrolyte will be more severe at higher current rates and the surface film will therefore be eroded more quickly, leaving the surface of the cathode materials directly in contact with the electrolyte. At this point, the acidic species in the electrolyte easily attacks the surface of the cathode and thereby decreases the discharge capacity enormously [17]. This decrease in capacity for the pristine sample plunged down to as low as 47 mA h g^{-1} at a current rate of 500 mA g^{-1}, while the ZrO_2 coated samples retained an average capacity of 76 mA h g^{-1}, with the highest value being observed for the 5 wt% sample. Additionally, the results for the cells with the best (5 wt% ZrO_2 coated) and worst (pristine) rate performance cycled at a cycling rate of 1 C within the same voltage range are shown in Fig. 4. The 5 wt% ZrO_2 coated sample showed an improved discharge capacity and cycle stability which were about 2 times higher than those of the pristine sample after 30 cycles. The shape of charge/discharge curves retained the monotonous decreasing nature of single phase reaction with a steady decrease in voltage at 1 C rate until 30 cycles for 5 wt% coated sample, while there is a rapid decrease in voltage with increasing cycle for pristine material (see Supplementary data, Fig. S1). It was shown that the ZrO_2 coating had higher fracture toughness than any other oxide coatings, such as Al_2O_3, TiO_2, B_2O_3 and SiO_2 [26]. The fracture toughness of ZrO_2 was calculated to be ~12 MPa m^{-2}, which is considered to be the highest value amongst ceramics [32]. It is therefore clear from the rate performance result that the ZrO_2 coating over the Li_2CoPO_4F material helps to retain the structure and electrochemical nature, including operation at high current rates and in the high voltage region. The ability of even a thin layer of ZrO_2 over the cathode surface to overcome the stress caused at high current rates is ascribed to the high fracture toughness of the material. Additionally, the formation of an inactive phase, unlike that observed in the case of $LiCoPO_4$ [33], may also be responsible for the poor performance of the pristine Li_2CoPO_4F material.

The cyclic voltammetry traces for the pristine and ZrO_2 coated samples were recorded between 2.0 and 5.1 V vs Li at a scan rate of 0.5 mV s^{-1}. The CV data shown in Fig. 5 exhibited a two stage lithium extraction process and a sharp insertion peak during the reverse scan for both the pristine and various coated samples. This reaction process and the peak positions correspond to the redox pattern of the $Co^{3+/2+}$ processes. The electrochemical oxidative area of the coated samples starts to increase from a ZrO_2 coating concentration of 1 wt% till it reaches 5 wt% and then starts to decrease. Similar behavior is observed during the reduction reaction. This explains the nature of the discharge capacities obtained for the coated samples. The pristine sample had the highest current response during charging as observed in the CV profile among the samples tested, which is due to the maximum electrolyte decomposition observed for the pristine material, and is similar to the additional charging capacity obtained during the charge/discharge studies. It is also clearly shown that the extraction of lithium was not complete till 5.1 V, as observed by the incomplete nature of the oxidation curve. These interpretations correlate well with the results obtained during the charge/discharge process.

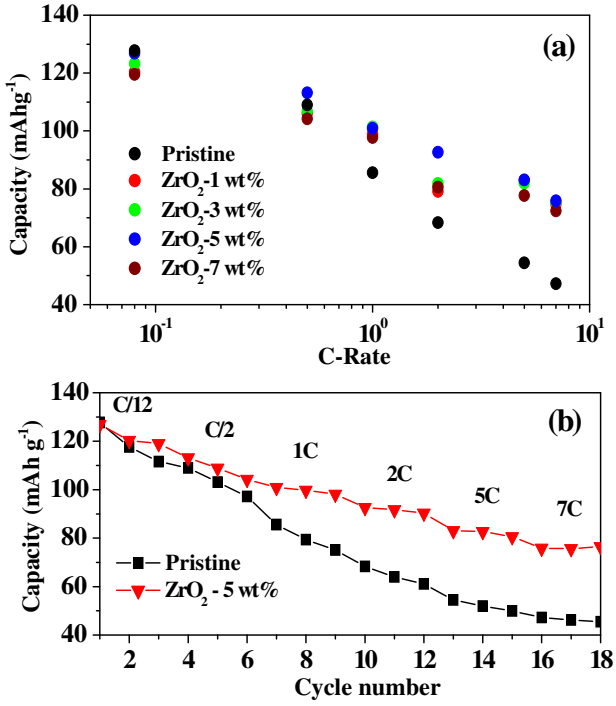

Fig. 3. (a) Rate performance of cells containing pristine Li_2CoPO_4F and Li_2CoPO_4F cathode materials coated with various amounts of ZrO_2 cycled between 2 and 5.1 V vs Li. (b) The cells containing the pristine and 5 wt% ZrO_2 coated Li_2CoPO_4F cathode materials were cycled for 3 cycles at each current rate.

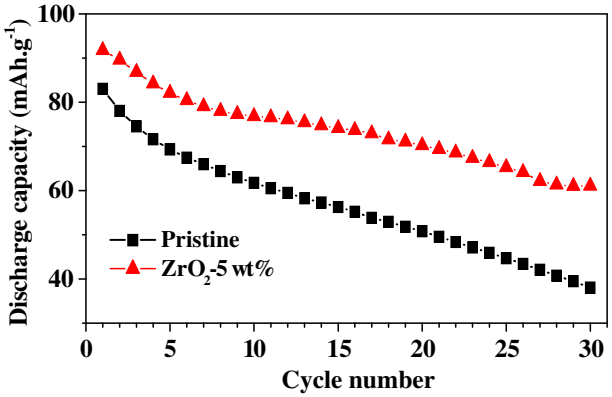

Fig. 4. Cycle performance of pristine and 5 wt% ZrO_2 coated Li_2CoPO_4F cathode materials at 1 C rate.

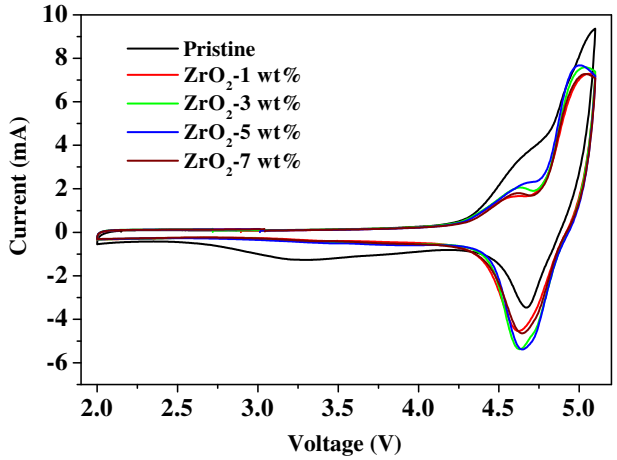

Fig. 5. Cyclic voltammetric study of cells containing pristine and various ZrO_2 coated Li_2CoPO_4F cathode materials between 2 and 5.1 V vs Li at 0.5 mV s^{-1} with lithium serving as both the counter and reference electrodes.

Impedance spectroscopy was carried out to check the influence of the resistance build up on the behavior of the cells containing the pristine and ZrO_2 coated Li_2CoPO_4F cathode active materials. The impedances of the cells were measured at open circuit potential in the frequency range of 100 kHz to 100 mHz and the results are presented in Fig. 6(a). All of the cells exhibit a semicircle in the high-medium frequency region and an inclined line at approximately 45° to the real axis in the low frequency region. The semicircle indicates the combined effect of the resistance due to the SEI film formed over the particle surface, the contact resistance between the particles and the charge transfer resistance along with the corresponding capacitance, while the inclined line corresponds to the lithium diffusion in the Li_2CoPO_4F cathodes associated with the Warburg impedance. A simplified equivalent circuit model was used to fit the experimental data (as shown in the inset of Fig. 6). R_s in the model is attributed to the ohmic resistance of the electrolyte; R_{ct} and Q correspond to the charge transfer resistance and constant phase element of the high-medium frequency semicircle, respectively, and Z_w indicates the Warburg impedance. The solution resistance calculated based on the intercept of the semicircle in the high frequency region with the real axis was about 5.5 Ω on average for all of the cells with the pristine and ZrO_2 coated Li_2CoPO_4F materials. R_{ct}, which is the difference between the intercept of the semicircle in the low frequency region and R_s, was at a maximum of 17 Ω for the pristine sample and at a minimum for the 5 wt% ZrO_2 coated sample. All of the other coated samples had higher resistances than the 5 wt% coated sample and, hence, the additional polarization of the cell before cycling itself is held responsible for its poor performance. The impedance build up during cycling was responsible for capacity degradation. Suppression of increase in impedance by the surface coating will lead to improved charge/discharge characteristics [40]. Impedance measurement at charged state for a cell can be useful in getting the information on the resistance for insertion of lithium ion back to the host cathode material. In this regard, EIS spectra were obtained for cells containing pristine and 5 wt% ZrO_2 coated LCPF after cycling. The cells were charged after 20 cycles and maintained at the upper cut off potential of 5.1 V till the current reached 1 C rate and, then, the impedance was measured. The 5 wt% ZrO_2 coated cell exhibited the lowest resistance even after cycling at 100 mA g^{-1}, as represented in Fig. 6(b). The reduction in resistance noted for Li_2CoPO_4F after coating with ZrO_2 improved the activity and performance of the Li_2CoPO_4F material, even under the highly acidic conditions formed during high rate cycling.

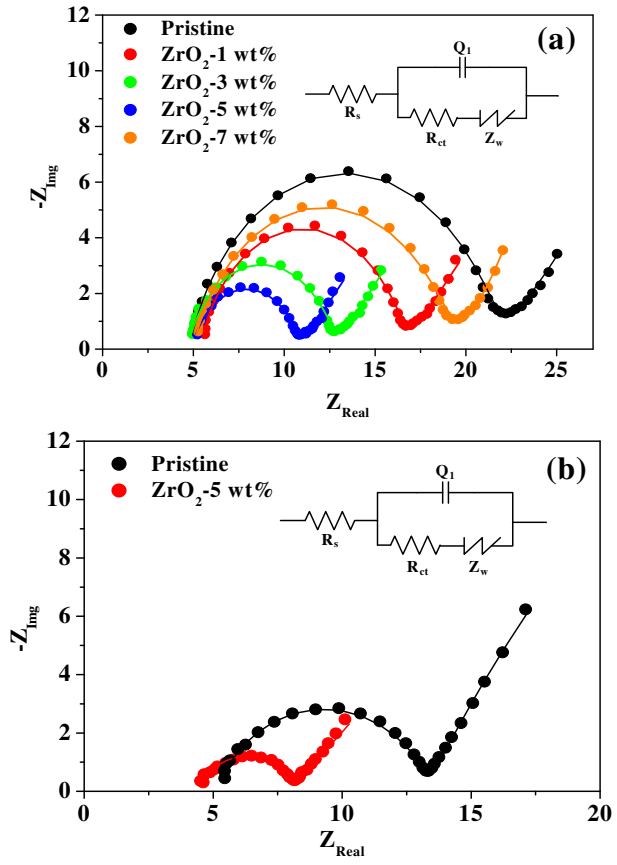

Fig. 6. Nyquist plots of pristine and ZrO_2 coated Li_2CoPO_4F cathode materials (a) at open circuit potential and (b) after cycling at 1 C rate. The symbols represent the experimental data and the continuous line corresponds to the fitted data obtained using the equivalent circuit model (inset).

Fig. 7(a) and (b) shows the SEM images of the pristine and 5 wt% ZrO_2 coated samples, respectively. It can be seen that the coating process resulted in a significant difference in the particle size and morphology of the pristine and coated active materials. The primary particles of the pristine Li_2CoPO_4F were in the range of 30–70 nm in size and the strong agglomeration of these primary particles to form bigger solids with a size as high as 3 μm was noticed. In order to achieve a uniform coating layer, the pristine Li_2CoPO_4F powder was sonicated for 30 min to develop a proper surface capable of adsorbing coating materials. This process led to the division of the large clumps of Li_2CoPO_4F particles into smaller ones and was further used for coating. The SEM observation of the particles after coating and subsequent heat treatment showed that they became separated during sonication and then became attached together during the heat treatment process after coating. Nevertheless, the powders retained a uniform spherical morphology. Furthermore, to confirm the nature and size of the coating layer, the 5 wt% ZrO_2 coated sample, having the highest capacity retention, was checked for the presence of the ZrO_2 coating layer using TEM and the results can be seen in Fig. 7(c). The highly magnified image shows a dark region comprising the synthesized active material and a less dark region representing the ZrO_2 coating layer. The synthesized Li_2CoPO_4F material shows crystal lattice spacing, while the coating layer does not. Hence, the coating layer is amorphous and forms a continuous layer with non-uniform thicknesses ranging from 3 to 10 nm. It was found that, in the case of ZrO_2, at moderate heating temperatures, the phase

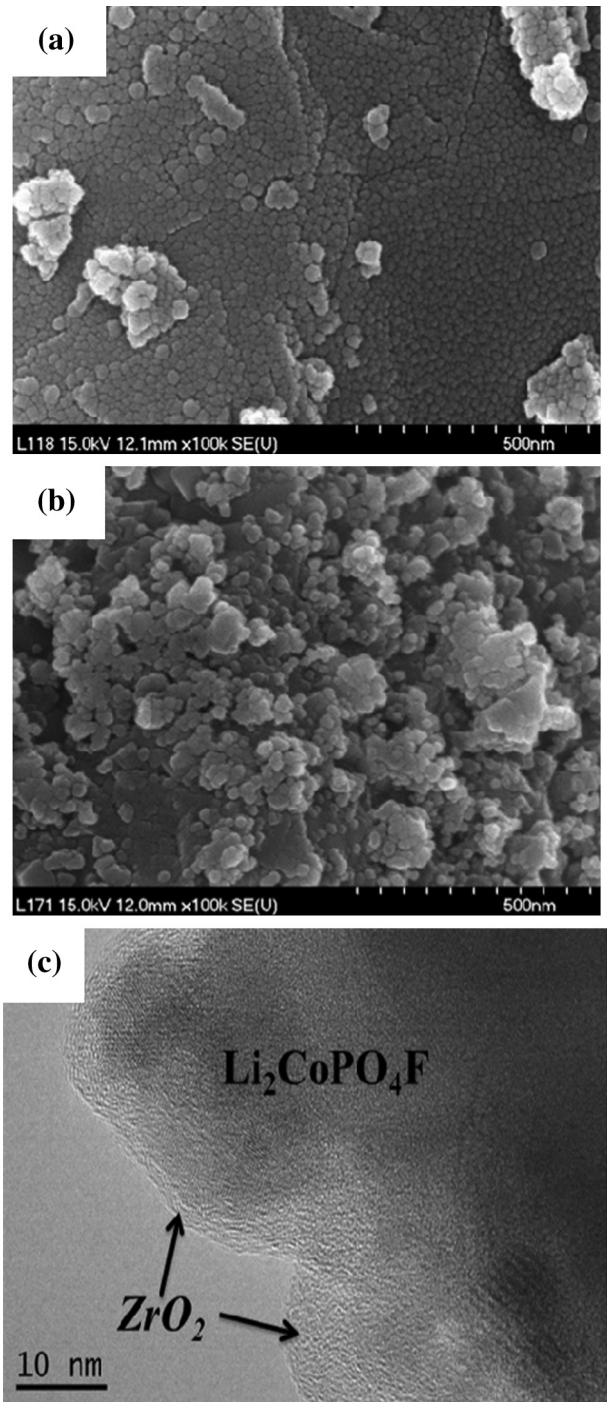

Fig. 7. SEM images of (a) pristine and (b) 5 wt% ZrO_2 coated Li_2CoPO_4F cathode materials. (c) The high resolution TEM image of the 5 wt% ZrO_2 coated sample shows the crystal lattice of Li_2CoPO_4F and the presence of an amorphous coating layer over the surface of the active material.

formed cannot be identified by X-ray diffraction and the solution with less than 10% dispersion was amorphous after calcination [34]. The results obtained from SEM and TEM correlated well with the nature of the coating determined by XRD. Also, it can be conjectured that the coating layer is responsible for protecting the surface of the primary particles from the attack of the electrolyte decomposition products and allows for the easier diffusion of Li ions during intercalation, thereby allowing the structure and morphology of the active material to be retained [35].

ZrO_2 acts as a bifunctional oxide which exhibits both acidic and basic properties, in contrast with other oxides such as MgO and SiO_2–Al_2O_3, the former being a solid base and the latter a solid acid [36]. This property helps ZrO_2 to retain its basic structure in the highly acidic environment caused by the formation of HF during electrochemical cycling and thus protects Li_2CoPO_4F. The PO_4 tetrahedral unit forms the basic structural unit of Li_2CoPO_4F. The IR spectrum of phosphate cathode materials is usually dominated by the vibrational spectra of the PO_4^{3-} polyanion. Generally, the FTIR spectra for phosphate tetrahedra shows a broad band between 900 and 1100 cm^{-1} for the stretching vibrations of the corresponding O–P–O bonding, while the bending vibrations are observed between 400 and 650 cm^{-1} [37]. Accordingly, the pristine and ZrO_2 coated samples were used for checking the effect of the ZrO_2 coating over the parent Li_2CoPO_4F active material. The IR spectra, as presented in Fig. 8, recorded between 400 and 4000 cm^{-1} showed the corresponding peaks at 1122, 1070, 1030 and 970 cm^{-1} for the symmetric–asymmetric stretching modes and 630, 585, 490, 470 and 428 cm^{-1} for the asymmetric–symmetric bending vibrations of the PO_4 tetrahedra. The IR spectra obtained for both the coated and uncoated samples showed no difference in their peak position and intensity variations. Hence, it is clearly understood from the FTIR spectrum and other structural characterizations such as XRD, SEM and TEM, that the ZrO_2 coating did not alter the fundamental behavior of Li_2CoPO_4F material and that the enhanced performance is due to the protective layer covering the surface of cathode material. The additional broad band between 3000 and 3800 cm^{-1} and shorter band at 1630 cm^{-1} noticed in the IR spectrum can be ascribed to the O–H adsorption band due to absorbed moisture [35].

The 5 wt% ZrO_2 coated sample was further tested at various rates for its operation at increased voltages of up to the upper cut off limit of 5.2 V vs Li while keeping the lower potential at 2 V vs Li and the electrochemical characteristics are given in Fig. 9(a) and (b). Reversible capacities of 144, 141, 122, 118 and 104 mA h g^{-1} were observed for C/12, C/2, 1 C, 2 C and 5 C rates, respectively. A capacity equivalent to complete extraction and insertion of one lithium unit at 10 mA g^{-1} from the Li_2CoPO_4F cathode material was achieved. The observed reduction in capacity when increasing the current rate can be ascribed to the increase in the charge transfer resistance and increased electrolyte decomposition. Although the cells used in the present study were the first of their kind used to test electrodes with a ZrO_2 coating at high voltages above 5.1 V [15,16,26,27], further increasing the voltage level caused the electrolyte to undergo extreme destruction and, hence, the tests were restricted to 5.2 V. In the cycling studies at a high voltage of 5.2 V, capacity retention of about 70% was

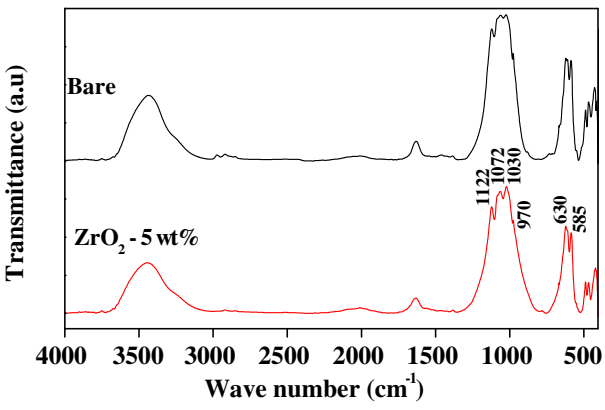

Fig. 8. FTIR spectra of pristine and 5 wt% ZrO_2 coated Li_2CoPO_4F cathode materials.

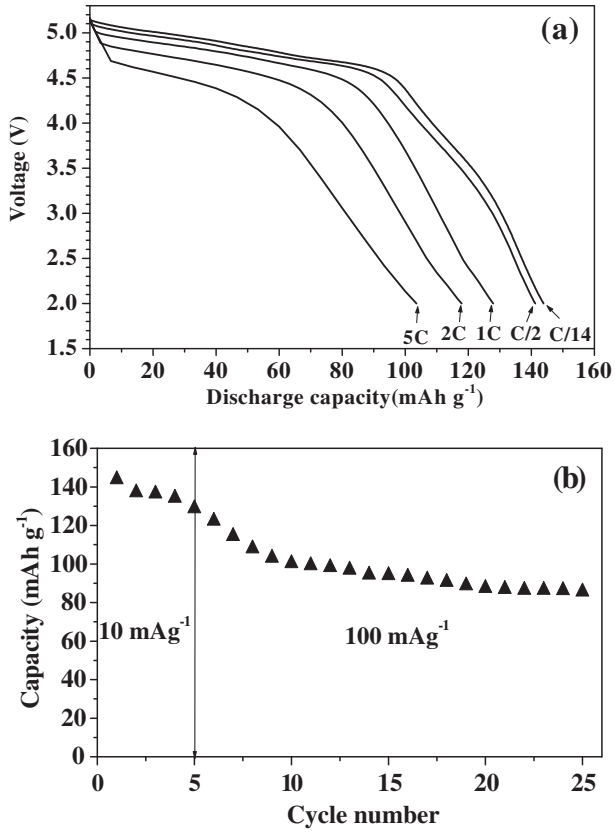

Fig. 9. (a) The characteristic discharge profiles of the 5 wt% ZrO_2 coated Li_2CoPO_4F cathode materials between 2 and 5.2 V at various rates and (b) the corresponding cycle lives of the cell at two current rates differing by a factor of 10.

observed, which is similar to the stability of the same material when charged to 5.1 V at a high current rate of 100 mA g^{-1} (1 C). This retention is comparable to that of the pristine Li_2CoPO_4F material, such that there is an increase in capacity of almost 70% even after 20 cycles at 1 C rate. The enhanced stability of the 5 wt % ZrO_2 coated Li_2CoPO_4F is due to the suppression of the increase in the charge transfer resistance during cycling. The stabilization of interface between the electrode and electrolyte with the utilization of increase in the BET surface area of 22% after coating, i.e., from 2.5 m^2 g^{-1} for the pristine to 3.05 m^2 g^{-1} for the 5 wt% ZrO_2 coated Li_2CoPO_4F, which has been observed in such metal oxide coatings [38], can also be responsible for enhanced performance.

4. Conclusion

The 5 wt% ZrO_2 coated Li_2CoPO_4F material showed better performance than the pristine active material. The coating did not change the bulk properties of the active material, but acted as a barrier between its surface and the electrolyte. It also increased the surface area, allowing for its effective utilization during the intercalation reactions. The TEM and XRD studies revealed that the coating layer was very thin and amorphous in nature, and hence, facilitated the movement of Li ions, causing an increase in capacity retention along with the improvement in cycle stability of Li_2CoPO_4F cathode material. The 5 wt% ZrO_2 coated Li_2CoPO_4F was tested up to 5.2 V vs Li and the full discharge capacity corresponding to one lithium intercalation reaction was obtained. The structure of the Li_2CoPO_4F active mass was retained even at a high current rate, which demonstrated the ability of the high fracture toughness ZrO_2 coating to inhibit electrolyte oxidation and reduce the surface reactivity of the Li_2CoPO_4F cathode with the electrolyte at high potentials. It also limited the diffusion of acids through the coating and reduced the exposure of the cathode surface to the electrolyte decomposition products, leading to the greater availability of the active materials for smooth intercalation reactions. The ZrO_2 coating can be used for retaining the performance of high voltage cathode materials, thereby extending the range of operation of lithium ion batteries.

Acknowledgements

This work was supported by the National Research Foundation of Korea Grant funded by the Korean Government (MEST) (NRF-2011-C1AAA001-0030538).

Appendix A. Supplementary data

Supplementary data related to this article can be found at http://dx.doi.org/10.1016/j.jpowsour.2012.12.010.

References

[1] M. Armand, J.M. Tarascon, Nature 451 (2008) 652–657.
[2] M. Stanley Whittingham, MRS Bull. 33 (2008) 411–419.
[3] A.K. Shukla, T. Prem Kumar, Curr. Sci. 94 (2008) 314–331.
[4] J.W. Fergus, J. Power Sources 195 (2010) 939–954.
[5] G.G. Amatucci, N. Pereira, J. Fluorine Chem. 128 (2007) 243–262.
[6] J. Barker, R.K.B. Gover, P. Burns, A. Bryan, M.Y. Saidi, J.L. Swoyer, J. Electrochem. Soc. 152 (2005) A1776–A1779.
[7] J. Barker, M.Y. Saidi, R.K.B. Gover, P. Burns, A. Bryan, J. Power Sources 174 (2007) 927–931.
[8] M. Dutreilh, C. Chevalier, M. El-Ghozzi, D. Avignant, J.M. Montel, J. Solid State Electrochem. 142 (1999) 1–5.
[9] B.L. Ellis, W.R.M. Makahnouk, W.N. Rowan-Weetaluktuk, D.H. Ryan, L.F. Nazar, Chem. Mater. 22 (2009) 1059–1070.
[10] Y. Makimura, L.S. Cahill, Y. Iriyama, G.R. Goward, L.F. Nazar, Chem. Mater. 20 (2008) 4240–4248.
[11] T.N. Ramesh, K.T. Lee, B.L. Ellis, L.F. Nazar, Electrochem. Solid-State Lett. 13 (2010) A43–A47.
[12] N. Recham, J.N. Chotard, J.C. Jumas, L. Laffont, M. Armand, J.M. Tarascon, Chem. Mater. 22 (2010) 1142–1148.
[13] S. Okada, M. Ueno, Y. Uebou, J.-i. Yamaki, J. Power Sources 146 (2005) 565–569.
[14] E. Dumont-Botto, C. Bourbon, S. Patoux, P. Rozier, M. Dolle, J. Power Sources 196 (2011) 2274–2278.
[15] J. Cho, T.-J. Kim, Y.J. Kim, B. Park, Electrochem. Solid-State Lett. 4 (2001) A159–A161.
[16] M.M. Thackeray, C.S. Johnson, J.S. Kim, K.C. Lauzze, J.T. Vaughey, N. Dietz, D. Abraham, S.A. Hackney, W. Zeltner, M.A. Anderson, Electrochem. Commun. 5 (2003) 752–758.
[17] J. Cho, Y.J. Kim, B. Park, Chem. Mater. 12 (2000) 3788–3791.
[18] J. Cho, Y.J. Kim, B. Park, J. Electrochem. Soc. 148 (2001) A1110–A1115.
[19] H. Liu, Z. Zhang, Z. Gong, Y. Yang, Solid State Ionics 166 (2004) 317–325.
[20] Z.R. Zhang, H.S. Liu, Z.L. Gong, Y. Yang, J. Power Sources 129 (2004) 101–106.
[21] Y. Iriyama, H. Kurita, I. Yamada, T. Abe, Z. Ogumi, J. Power Sources 137 (2004) 111–116.
[22] Z.R. Zhang, H.S. Liu, Z.L. Gong, Y. Yang, J. Electrochem. Soc. 151 (2004) A599–A603.
[23] M. Mladenov, R. Stoyanova, E. Zhecheva, S. Vassilev, Electrochem. Commun. 3 (2001) 410–416.
[24] Y.K. Sun, K.J. Hong, J. Prakash, K. Amine, Electrochem. Commun. 4 (2002) 344–348.
[25] Y.K. Sun, Y.S. Lee, M. Yoshio, K. Amine, Electrochem. Solid-State Lett. 5 (2002) A99–A102.
[26] Y.J. Kim, J. Cho, T.-J. Kim, B. Park, J. Electrochem. Soc. 150 (2003) A1723–A1725.
[27] G.G. Amatucci, A. Blyr, C. Sigala, P. Alfonse, J.M. Tarascon, Solid State Ionics 104 (1999) 13–25.
[28] D. Wang, J. Xiao, W. Xu, Z. Nie, C. Wang, G. Graff, J.-G. Zhang, J. Power Sources 196 (2011) 2241–2245.
[29] N.V. Kosova, E.T. Devyatkina, A.B. Slobodyuk, Solid State Ionics 225 (2012) 570–574.
[30] S.M. Lee, S.H. Oh, J.P. Ahn, W.I. Cho, H. Jang, J. Power Sources 159 (2006) 1334–1339.
[31] N.N. Bramnik, K. Nikolowski, C. Baehtz, K.G. Bramnik, H. Ehrenberg, Chem. Mater. 19 (2007) 908–915.

[32] W.D. Callister, Materials Science and Engineering: An Introduction, John Wiley & Sons, New York, 1997.
[33] N.N. Bramnik, K. Nikolowski, D.M. Trots, H. Ehrenberg, Electrochem. Solid-State Lett. 11 (2008) A89–A93.
[34] Y. Tsutomu, Catal. Today 20 (1994) 199–218.
[35] Z. Chen, Y. Qin, K. Amine, Y.K. Sun, J. Mater. Chem. 20 (2010) 7606–7612.
[36] X. Bo-Qing, Y. Tsutomu, T. Kozo, Chem. Lett. 17 (1988) 1663–1666.
[37] K. Nakamoto, Infrared and Raman Spectra of Inorganic and Coordination Compounds, Wiley and Sons, New York, 1978.
[38] D. Li, Y. Kato, K. Kobayakawa, H. Noguchi, Y. Sato, J. Power Sources 160 (2006) 1342–1348.
[39] S. Amaresh, G.J. Kim, K. Karthikeyan, V. Aravindan, K.Y. Chung, B.W. Cho, Y.S. Lee, Phys. Chem. Chem. Phys. 14 (2012) 11904–11909.
[40] J.M. Zheng, Z.R. Zhang, X.B. Wu, Z.X. Dong, Z. Zhu, Y. Yang, J. Electrochem. Soc. 155 (10) (2008) A775–A782.